

# Concomitant appearance of conductivity and superconductivity in (111) LaAlO<sub>3</sub>/SrTiO<sub>3</sub> interface with metal capping

R. S. Bisht,<sup>1</sup> M. Mograbi,<sup>1</sup> P. K. Rout,<sup>1</sup> G. Tuvia,<sup>1</sup> Hye-Ok Yoon,<sup>2,3</sup> A. G. Swartz,<sup>2,3</sup> H. Y. Hwang,<sup>2,3</sup> and Y. Dagan<sup>1,\*</sup>

<sup>1</sup>*Raymond and Beverly Sackler School of Physics and Astronomy, Tel-Aviv University, Tel Aviv, 6997801, Israel*

<sup>2</sup>*Department of Applied Physics, Geballe Laboratory for Advanced Materials, Stanford University, 476 Lomita Mall, Stanford, CA 94305, USA*

<sup>3</sup>*Stanford Institute for Materials and Energy Sciences, SLAC National Accelerator Laboratory, Menlo Park, California 94025, USA*

(Dated: January 27, 2023)

In polar-oxide interfaces, a certain number of monolayers (ML) is needed for conductivity to appear. This threshold for conductivity is explained by the accumulation of sufficient electric potential to initiate charge transfer to the interface. Here we study the (111) SrTiO<sub>3</sub>/LaAlO<sub>3</sub> interface where a critical thickness of nine epitaxial LaAlO<sub>3</sub> ML is required to turn the interface from insulating to conducting and even superconducting. We show that this critical thickness decreases to 3ML when depositing a cobalt over-layer (capping) and 6ML for platinum capping. The latter result contrasts with the (100) interface where platinum capping increases the critical thickness beyond that of the bare interface. These results suggest that the work function of the metallic capping plays an important role in both interfaces. Interestingly, for (111) SrTiO<sub>3</sub>/LaAlO<sub>3</sub>/Metal interfaces conductivity appears concomitantly with superconductivity in contrast with the SrTiO<sub>3</sub>/LaAlO<sub>3</sub>/Metal interface with LaAlO<sub>3</sub> layer smaller than four ML (unit-cells), which are conducting but not superconducting. We suggest that this difference is related to the different sub-bands involved in conductivity for the (111) interfaces, comparing to the (100) interfaces. Our findings can be useful for superconducting devices made of such interfaces.

The interface between LaAlO<sub>3</sub> and SrTiO<sub>3</sub> exhibits two-dimensional conductivity [1], superconductivity [2], magnetism [3–8], metal-insulator transition [9], tunable Rashba spin-orbit interaction [10, 11], quantum hall states [12, 13], and one-dimensional conductivity [14, 15]. While the (100) SrTiO<sub>3</sub>/LaAlO<sub>3</sub> interface received significant scientific attention, the (111) interface remains less explored.

In (111) SrTiO<sub>3</sub>/LaAlO<sub>3</sub> interface three distinct triangular Ti layers form one monolayer [16, 17]. In bulk, the crystal field results in a splitting of the 3d orbitals into  $e_g$  and three degenerate  $t_{2g}$  manifolds that are further split due to the trigonal symmetry at the interface into  $a_{1g}$  and  $e'_g$  orbitals. The six-fold symmetry of the titanium layer is reflected in the transport properties [18]. The symmetry is further reduced due to the structural transition of SrTiO<sub>3</sub> and the interface is predicted to host exotic superconductivity [19] and topological states [20].

Four monolayers of LaAlO<sub>3</sub> are needed for the formation of two-dimensional electron system (2DES) at the (100) SrTiO<sub>3</sub>/LaAlO<sub>3</sub> interface [9]. For the (111) interface, the critical thickness for conductivity is nine monolayers (ML) [16]. The (111) 2DES also exhibits superconductivity [21], with a link between superconductivity and spin-orbit interaction [22]. Importantly, upon carrier depletion with negative gate voltage superconductivity transitions into a Bose-insulating state [23]. This behavior contrasts with the (100) interface where a weaker insulating state is observed for negative gate biases [24, 25].

For spin injection and low voltage transistor applications the barrier produced by the minimal four monolayers of LaAlO<sub>3</sub> required for conductivity at the bare (100) interface or by the nine monolayers at the (111) interface is relatively strong. Recent first principle calculations [26] and experimental studies of various metal capping on (100) interfaces (SrTiO<sub>3</sub>/LaAlO<sub>3</sub>/Metal) [27, 28] show that the critical thickness for the onset of conductivity,  $t_{LAO}$ , can be reduced relative to the bare interface.  $t_{LAO}$  increases with the work function. Here we study the problem of critical thickness for conductivity for (111) interfaces. We have also expanded our research to the superconducting properties of both (100) and (111) SrTiO<sub>3</sub>/LaAlO<sub>3</sub>/metal interfaces. We find that upon capping the LaAlO<sub>3</sub> in (111) SrTiO<sub>3</sub>/LaAlO<sub>3</sub> interface with cobalt (Co) and platinum (Pt),  $t_{LAO}$  has been suppressed from 9 ML to 3 ML and 6 ML, respectively. Furthermore, once the (111) interface becomes conducting, it also becomes superconducting at low temperatures. This contrasts with the (100) interface where superconductivity is not observed in SrTiO<sub>3</sub>/LaAlO<sub>3</sub>/Metal interfaces with reduced  $t_{LAO}$ . We suggest that for (111) interface, the bands responsible for conductivity and superconductivity are the same while for (100) conductivity appears first in the  $d_{xy}$  type bands, which are not superconducting [17, 29].

Epitaxial LaAlO<sub>3</sub> films with different thickness were grown on Ti and TiO<sub>2</sub> terminated atomically smooth (111) and (100) SrTiO<sub>3</sub> substrates respectively at an oxygen pressure of  $1 \times 10^{-4}$  Torr and temperature 780°C using pulsed laser deposition. The thickness was in-situ monitored by reflection high energy electron diffraction

\* Corresponding author: yodagan@tauex.tau.ac.il

(RHEED). The samples were then transferred to a magnetron sputtering chamber where they were pre-annealed for two minutes at  $200^{\circ}\text{C}$  and at a pressure of  $1 \times 10^{-8}$  Torr to remove surface contaminants. Metallic layers of  $\approx 3$  nm of platinum (Pt), silver (Ag), or cobalt (Co) were deposited in an argon atmosphere at room temperature. For the latter, we used an additional 3 nm  $\text{AlO}_x$  to prevent oxidation. Wire bonding was used to connect to the sample electrically. In this configuration, the measured resistance is either a parallel combination of the metal cap resistance and the 2DES at the conducting  $\text{SrTiO}_3/\text{LaAlO}_3$  interface or only the metallic cap in the absence of 2DES. We demonstrate this by measuring the transverse resistance  $R_{xy}$  i.e., the Hall signal of the (111)  $\text{SrTiO}_3/\text{LaAlO}_3/\text{Co}/\text{AlO}_x$  interface for 4  $\text{LaAlO}_3$  ML, as shown in Fig.1. While for positive gate voltage, the 2DES dominates and exhibits signal resembling the (111)  $\text{SrTiO}_3/\text{LaAlO}_3$  interface [22] when depleting the 2DES by negative gate voltage, the contribution of Co predominates as manifested in an anomalous-Hall signal confirming the presence of two parallel channels for conduction. This behavior is similar to (100) with cobalt capping [28].

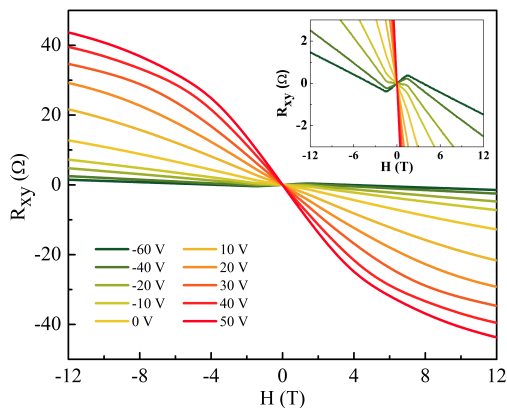


FIG. 1. Transverse resistance of (111) $\text{SrTiO}_3/\text{LaAlO}_3/\text{Co}/\text{AlO}_x$  for 4 ML  $\text{LaAlO}_3$  as a function of a perpendicular magnetic field at different gate voltages. The inset focuses on the negative gate voltage regime. The observed anomalous-Hall signal demonstrates the predominance of the Co layer properties in this regime. This is in contrast to the higher carrier density regime where the 2DES dominates.

The transport studies conducted on (111)  $\text{SrTiO}_3/\text{LaAlO}_3/\text{Co}/\text{AlO}_x$  interface show a reduction of  $\text{LaAlO}_3$  critical thickness for the onset of 2DES conductivity from 9 ML to 3 ML. In Fig.2 (a) we show the sheet resistance of (111) $\text{SrTiO}_3/\text{LaAlO}_3/\text{Co}/\text{AlO}_x$  as a function of  $\text{LaAlO}_3$  thickness at 40 K. For  $\text{LaAlO}_3$  thickness below 3 ML, the resistance increases by nearly five times. This indicates that 3 ML is the critical thickness of  $\text{LaAlO}_3(t_{LAO})$  for the onset of conductivity with Co capping. To verify that a 2DES is

formed parallel to the metallic layer, we measured the resistance versus back gate voltage. For a thin metallic layer parallel to a 2DES, one expects gate dependent resistance due to the dominating contribution of 2DES. On the other hand, in the absence of a 2DES parallel to a metallic layer we expect the gate dependence of the resistance to be immeasurably small due to the substantial carrier density in the metal. Fig.2 (b) shows the gate dependence of (111)  $\text{SrTiO}_3/\text{LaAlO}_3/\text{Co}/\text{AlO}_x$  for 1 and 3  $\text{LaAlO}_3$  ML. For the sample with a single  $\text{LaAlO}_3$  ML, the normalized resistance ( $R/R_{(-60V)}$ ) is flat as a function of gate voltage, suggesting the absence of 2DES at the  $\text{SrTiO}_3/\text{LaAlO}_3$  interface. For 3 ML  $\text{LaAlO}_3$ , the data show a significant gate dependence, suggesting the formation of 2DES at (111) $\text{SrTiO}_3/\text{LaAlO}_3$  interface. We interpret the saturation of the resistance at negative gate voltage as a result of depletion of the 2DES and dominance of the Co capping layer. We conclude that  $t_{LAO}$  becomes 3 ML upon Co capping for (111) interface.

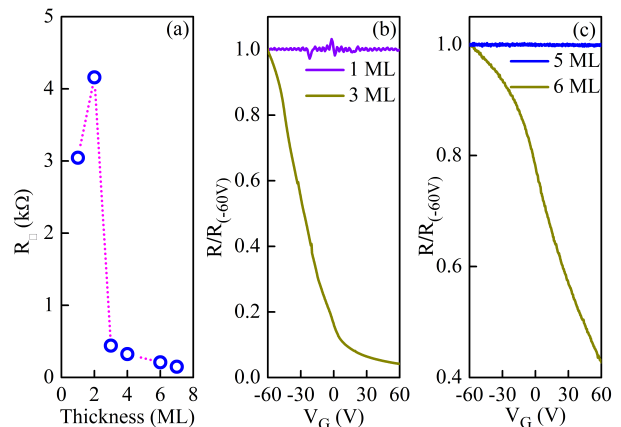


FIG. 2. (a) The sheet resistance ( $R_{\square}$ ) of (111)  $\text{SrTiO}_3/\text{LaAlO}_3/\text{Co}/\text{AlO}_x$  at 40 K as a function of  $\text{LaAlO}_3$  thickness, an abrupt drop in the resistance at 3 ML indicates that this is the critical thickness for the formation of 2DES at the  $\text{SrTiO}_3/\text{LaAlO}_3$  interface. Note: The measured samples were not patterned, the geometrical factor for the sheet resistance calculation is within an error bar of  $\pm 10\%$ . (b) The gate dependence of the normalized resistance ( $R/R_{(-60V)}$ ) for (111)  $\text{SrTiO}_3/\text{LaAlO}_3/\text{Co}/\text{AlO}_x$  with  $\text{LaAlO}_3$  thickness of 1 and 3 monolayers. (c) The gate dependence of normalized resistance ( $R/R_{(-60V)}$ ) for (111)  $\text{SrTiO}_3/\text{LaAlO}_3/\text{Pt}$  for  $\text{LaAlO}_3$  thickness of 5 and 6 monolayers.

Previous studies on the metal-capped (100)  $\text{SrTiO}_3/\text{LaAlO}_3$  interface show that the critical thickness increases with the work-function of the metal-capping layer [26]. To understand the role of the work function in (111) interfaces, we carried out experiments with Pt capping. The work-function of platinum is generally higher than that of Co [30]. Surprisingly, we found that unlike the (100) interface, Pt capping also

reduces  $t_{LAO}$  from 9 ML to 6 ML. This is demonstrated in Fig.2(c), where we show the gate dependence of (111)SrTiO<sub>3</sub>/LaAlO<sub>3</sub>/Pt for 5 and 6 LaAlO<sub>3</sub> ML. The absence of gate dependence for 5ML and the strong gate dependence for 6ML suggests that  $t_{LAO}$  with Pt cap is 6 ML. In Figure S1 (Supplemental information), we also show the gate dependence of the extracted sheet resistance of 2DES for (111)SrTiO<sub>3</sub>/LaAlO<sub>3</sub>/Co/AlO<sub>x</sub> and (111)SrTiO<sub>3</sub>/LaAlO<sub>3</sub>/Pt for 3 ML and 6 ML of LaAlO<sub>3</sub>.

While suppression of  $t_{LAO}$  upon Co capping is observed for both the (111) and (100) SrTiO<sub>3</sub>/LaAlO<sub>3</sub> interfaces, a reduction of  $t_{LAO}$  upon Pt capping is observed only for (111) interface, whereas an increase in  $t_{LAO}$  is found for the Pt capped (100) interface [28]. A plausible explanation for that is the dependence of the effective work-function on the surface properties[31].

The data presented above unveil that  $t_{LAO}$  has a strong dependence on the work function. But how does metal capping affect superconductivity for the (100) and (111) interfaces? To address this question, we cooled down our samples in a dilution refrigerator. Surprisingly, we find that all the (111) samples, which show conductivity on metal capping, also show superconductivity. In table 1 and S1 (Supplemental information), we summarize the properties of the (100) and (111) interfaces with various LaAlO<sub>3</sub> thickness and different metal capping. Fig.3 displays the normalized resistance ( $R/R_{(0.5K)}$ ) as a function of temperature for different (100) and (111) interfaces at the critical thickness  $t_{LAO}$  with Co and Pt capping. As shown previously in Fig.1, the Co layer indeed shows an anomalous hall effect, but for such a thin cobalt film, one expects the magnetic coupling to be extremely short with a negligible effect on the 2DES. Nevertheless, to eliminate the possibility that the close proximity ( $12\text{\AA}$ ) of the ferromagnetic Co to the interface is responsible for the absence of superconductivity in the (100) SrTiO<sub>3</sub>/LaAlO<sub>3</sub>/Co/AlO<sub>x</sub>, we measured (non-magnetic) Ag capped (100) interface with 3 ML of LaAlO<sub>3</sub>, which also shows no superconductivity. In Figure S2 (Supplemental information), we show the temperature and gate bias dependence of the resistance for Ag capped (100) interface.

To make sure that the observed superconductivity is a two-dimensional (2D) interfacial effect and not a spurious one resulting from the sputtering process, we studied the temperature dependence of the perpendicular and parallel critical field. We show in the supplementary information that they both follow the expected 2D Ginzburg-Landau temperature dependence (See Figure S3 of supplemental information).

In Fig.4 we show the behavior of the critical temperature and critical fields as a function of gate voltage for Co and Pt capped (111) interface. The dome shaped gate dependence and the values of  $T_c$ , the perpendicular critical field  $H_{\perp}$ , and the parallel critical field  $H_{\parallel}$  are similar to the bare (111) SrTiO<sub>3</sub>/LaAlO<sub>3</sub> interface [17, 22].

The important findings we report here are the sup-

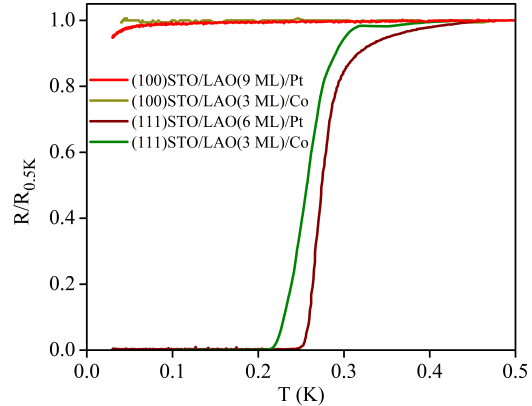


FIG. 3. The normalized resistance ( $R/R_{(0.5K)}$ ) of (100) SrTiO<sub>3</sub>/LaAlO<sub>3</sub>(3ML)/Co/AlO<sub>x</sub>, (100)SrTiO<sub>3</sub>/LaAlO<sub>3</sub>(9ML)/Pt, (111) SrTiO<sub>3</sub>/LaAlO<sub>3</sub>(3ML)/ Co/AlO<sub>x</sub>, and (111) SrTiO<sub>3</sub>/LaAlO<sub>3</sub>(6ML)/Pt. The LaAlO<sub>3</sub>/SrTiO<sub>3</sub>(111) interfaces capped with Co and Pt show a superconducting transition and the corresponding critical thickness of LAO is 3 and 6 Monolayer respectively.

pression of  $t_{LAO}$  for (111) interfaces both with Co and with Pt capping. This is in contrast with the (100) interface where  $t_{LAO}$  with Pt capping has been shown to increase relative to the bare interface[28]. Furthermore, once conductivity appears by either Pt or Co capping on (111) SrTiO<sub>3</sub>/LaAlO<sub>3</sub> interfaces (with LaAlO<sub>3</sub> thickness larger than or equals to  $t_{LAO}$ ) superconductivity is observed at low temperatures. This is not the case for (100) SrTiO<sub>3</sub>/LaAlO<sub>3</sub>/metal (Fig.3).

It has been shown theoretically that the work function of the capping metal as well as the size and direction of the internal electric dipole in the LaAlO<sub>3</sub> layer affect the degree of charge transfer from the metal to the Ti 3d bands at the interface [26] and consequently influence  $t_{LAO}$ . These predictions have been verified experimentally [28]. A naive inspection of the internal dipole field at the (111) SrTiO<sub>3</sub>/LaAlO<sub>3</sub> interface shows that it is in-fact opposite to that of (100) counterpart [16]. It is known that the different surface adsorbates can modify the electronic properties of the SrTiO<sub>3</sub>/LaAlO<sub>3</sub> interface[32]. In addition, For metals, the effective work function strongly depends on the number of surface dipoles. The latter depends on the surface reconstructions, as well as on the atmospheric adsorbates. It is, therefore, possible that the deposited Pt can have some additional surface effects on the (111) orientation compared to the (100) orientation. This modification of the electrostatic boundary conditions may be at the origin of the suppression of  $t_{LAO}$  with Pt capping for the (111) interface.

The other important observation is the presence of superconductivity in the metal-capped (111) interface in

TABLE I. Summary of the different samples measured for various thickness of  $\text{LaAlO}_3$  upon different metal capping and corresponding nature of the interface. Note: For (100) interface one monolayer corresponds to one unit-cell (see also table S1 (Supplemental information) for more samples).

Interface	Metal layer	Thickness (ML)	Conducting	Super-Conducting
(111)	Co	2	No	No
(111)	Co	3	Yes	Yes
(100)	Co	2	Yes	No
(100)	Co	3	Yes	No
(111)	Pt	5	No	No
(111)	Pt	6	Yes	Yes
(100)	Pt	9	Yes	No
(100)	Ag	3	Yes	No

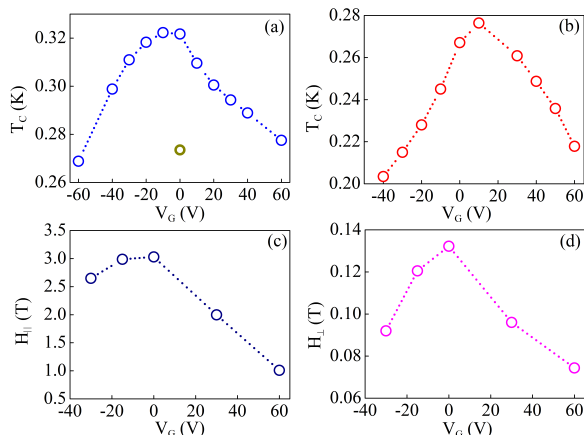


FIG. 4. (a) The critical temperature ( $T_c$ ) of (111)  $\text{SrTiO}_3/\text{LaAlO}_3(6\text{ML})/\text{Pt}$  interface, the dark yellow circle shows the  $T_c$  of the as cooled film. (b), (c) and (d) are superconducting critical temperature, perpendicular critical field and parallel critical field respectively of the (111)  $\text{SrTiO}_3/\text{LaAlO}_3(3\text{ML})/\text{Co}/\text{AlO}_x$  interface as a function of gate voltage. The values of these critical parameters are in good agreement with that of the uncapped interface. Note:  $T_c$  is defined as a temperature where the value of resistance drops by 50% of its value at 0.5 K.

contrast to the (100) interface as demonstrated in Table 1 and in table S1 in the supplementary part.

How can we understand the robustness of superconductivity in (111) interfaces? Previous experimental studies on (111)  $\text{SrTiO}_3/\text{LaAlO}_3$  interfaces show that even at strong negative gate voltages superconductivity remains intact [22, 23]. On the theory side, the curvature of the Fermi contour changes quickly upon charge accumulation, and both the conducting and superconducting

bands get an equal contribution from the three degenerate  $t_{2g}$  orbitals[17]. By contrast, for (100) interface, there are distinct less mobile, non-superconducting band and a mobile superconducting band due to the very different effective masses of the light  $d_{xy}$  and heavy  $d_{yz}$ ,  $d_{xz}$  bands. It is possible that the inter-band repulsion [29] results in shifting the second band to higher energy leaving only the metallic state. On the (111) interface, the splitting of  $t_{2g}$  orbitals occurs due to the crystal field. The crystal field splitting may be sensitive to the details of the interface. For example, the lowermost band is  $a_{1g}$  in (111)  $\text{SrTiO}_3/\text{LaAlO}_3$ , but it is the  $e'_g$  in doped surface of (111)  $\text{SrTiO}_3$  crystal[33]. It is possible that by metallic capping, the sign of the crystal field changes and the superconducting  $e'_g$  bands become lower in energy. In this case, one or two mobile bands will be occupied at all gate voltages and one should see both conductivity and superconductivity.

To summarize, capping of Co and Pt on (111) $\text{SrTiO}_3/\text{LaAlO}_3$  interface reduces the critical thickness for the onset of conductivity. Importantly, all conducting (111) interfaces are also superconducting at low temperatures. Our findings suggest that proper choice of metal on top of the  $\text{LaAlO}_3$  barrier can tune the barrier strength for various applications such as superconducting tunneling devices and ferromagnetic tunnel junction.

RSB and MM contributed equally to this work.

## ACKNOWLEDGMENTS

We thank Moshe Goldstein and Udit Khanna for useful discussions. This research was supported by the Binational Science Foundation under grant 2014047 and by the Israel Science Foundation under grant : 382/17.

[1] A. Ohtomo and H. Y. Hwang, Nature **427**, 423 (2004).  
 [2] N. Reyren, S. Thiel, A. D. Caviglia, L. F. Kourkoutis, G. Hammerl, C. Richter, C. W. Schneider, T. Kopp, A.-

S. Rüetschi, D. Jaccard, et al., Science **317**, 1196 (2007).  
 [3] A. Brinkman, M. Huijben, M. van Zalk, J. Huijben, U. Zeitler, J. C. Maan, W. G. van der Wiel, G. Rijnders,

- D. H. A. Blank, and H. Hilgenkamp, *Nature Materials* **6**, 493 (2007).
- [4] M. Sachs, D. Rakhmilevitch, M. Ben Shalom, S. Shefler, A. Palevski, and Y. Dagan, *Physica C: Superconductivity and its applications* **470**, S746 (2010).
- [5] J. A. Bert, B. Kalisky, C. Bell, M. Kim, Y. Hikita, H. Y. Hwang, and K. A. Moler, *Nature Physics* **7**, 767 (2011).
- [6] A. Ron, E. Maniv, D. Graf, J.-H. Park, and Y. Dagan, *Phys. Rev. Lett.* **113**, 216801 (2014).
- [7] S. Seri and L. Klein, *Phys. Rev. B* **80**, 180410 (2009).
- [8] J.-S. Lee, Y. Xie, H. Sato, C. Bell, Y. Hikita, H. Hwang, and C.-C. Kao, *Nature Materials* **12**, 703 (2013).
- [9] S. Thiel, G. Hammerl, A. Schmehl, C. W. Schneider, and J. Mannhart, *Science* **313**, 1942 (2006).
- [10] M. Ben Shalom, M. Sachs, D. Rakhmilevitch, A. Palevski, and Y. Dagan, *Phys. Rev. Lett.* **104**, 126802 (2010).
- [11] A. Caviglia, M. Gabay, S. Gariglio, N. Reyren, C. Cancellieri, and J.-M. Triscone, *Phys. Rev. Lett.* **104**, 126803 (2010).
- [12] Y. Xie, C. Bell, M. Kim, H. Inoue, Y. Hikita, and H. Y. Hwang, *Solid state communications* **197**, 25 (2014).
- [13] F. Trier, G. E. Prawiroatmodjo, Z. Zhong, D. V. Christensen, M. von Soosten, A. Bhowmik, J. M. G. Lastra, Y. Chen, T. S. Jespersen, and N. Pryds, *Phys. Rev. Lett.* **117**, 096804 (2016).
- [14] A. Ron and Y. Dagan, *Phys. Rev. Lett.* **112**, 136801 (2014).
- [15] M. Briggeman, M. Tomczyk, B. Tian, H. Lee, J.-W. Lee, Y. He, A. Tylan-Tyler, M. Huang, C.-B. Eom, D. Pekker, et al., *Science* **367**, 769 (2020).
- [16] G. Herranz, F. Sánchez, N. Dix, M. Scigaj, and J. Fontcuberta, *Sci. Rep.* **2**, 758 (2012).
- [17] U. Khanna, P. K. Rout, M. Mograbi, G. Tuvia, I. Leermakers, U. Zeitler, Y. Dagan, and M. Goldstein, *Phys. Rev. Lett.* **123**, 036805 (2019).
- [18] P. K. Rout, I. Agireen, E. Maniv, M. Goldstein, and Y. Dagan, *Phys. Rev. B* **95**, 241107 (2017).
- [19] M. Hecker and J. Schmalian, *npj Quantum Materials* **3**, 1 (2018).
- [20] D. Doennig, W. E. Pickett, and R. Pentcheva, *Phys. Rev. Lett.* **111**, 126804 (2013).
- [21] A. M. R. V. L. Monteiro, D. J. Groenendijk, I. Groen, J. de Bruijkere, R. Gaudenzi, H. S. J. van der Zant, and A. D. Caviglia, *Phys. Rev. B* **96**, 020504 (2017).
- [22] P. K. Rout, E. Maniv, and Y. Dagan, *Phys. Rev. Lett.* **119**, 237002 (2017).
- [23] M. Mograbi, E. Maniv, P. K. Rout, D. Graf, J.-H. Park, and Y. Dagan, *Phys. Rev. B* **99**, 094507 (2019).
- [24] A. D. Caviglia, S. Gariglio, N. Reyren, D. Jaccard, T. Schneider, M. Gabay, S. Thiel, G. Hammerl, J. Mannhart, and J.-M. Triscone, *Nature* **456**, 624 (2008).
- [25] Z. Chen, A. G. Swartz, H. Yoon, H. Inoue, T. A. Merz, D. Lu, Y. Xie, H. Yuan, Y. Hikita, S. Raghu, et al., *Nature communications* **9**, 1 (2018).
- [26] R. Arras, V. G. Ruiz, W. E. Pickett, and R. Pentcheva, *Phys. Rev. B* **85**, 125404 (2012).
- [27] E. Lesne, N. Reyren, D. Doennig, R. Mattana, H. Jaffrès, V. Cros, F. Petroff, F. Choueikani, P. Ohresser, R. Pentcheva, et al., *Nature Communications* **5** (2014).
- [28] D. C. Vaz, E. Lesne, A. Sander, H. Naganuma, E. Jacquet, J. Santamaria, A. Barthélémy, and M. Bibes, *Advanced Materials* **29**, 1700486 (2017).
- [29] E. Maniv, M. B. Shalom, A. Ron, M. Mograbi, A. Palevski, M. Goldstein, and Y. Dagan, *Nature Communications* **6**, 8239 (2015).
- [30] H. B. Michaelson, *J. Appl. Phys.* **48**, 4729 (1977).
- [31] M. Mrovec, J.-M. Albina, B. Meyer, and C. Elsässer, *Phys. Rev. B* **79**, 245121 (2009).
- [32] Y. Xie, Y. Hikita, C. Bell, and H. Y. Hwang, *Nature Communications* **2**, 494 (2011).
- [33] G. M. De Luca, R. Di Capua, E. Di Gennaro, A. Sambri, F. M. Granozio, G. Ghiringhelli, D. Betto, C. Piamonteze, N. B. Brookes, and M. Salluzzo, *Phys. Rev. B* **98**, 115143 (2018).

## Supplemental Material for Concomitant appearance of conductivity and superconductivity in (111) LaAlO<sub>3</sub>/SrTiO<sub>3</sub> interface on metal capping

### S1: Sheet Resistance of two dimensional electron system without Capping

The sheet resistance of the two dimensional electron system (2DES) without capping was extracted from the analysis of the parallel resistance model as given in the equation 1. Where  $R_{Measured}$ ,  $R_{Metal-Overlayer}$ , and  $R_{2DES}$  is the experimentally measured resistance of the parallel conducting channel, resistance of metal overlayer, and resistance of the 2DES respectively. In our analysis we assumed  $R_{metal-capping} = R_{Measured}$  at strong negative gate voltages. Figure S1 represents the extracted sheet resistance of the 2DES for (111)SrTiO<sub>3</sub>/LaAlO<sub>3</sub>/Co/AlO<sub>x</sub> and (111)SrTiO<sub>3</sub>/LaAlO<sub>3</sub>/Pt samples for 3 and 6 ML LaAlO<sub>3</sub> as a function of gate voltages. The diverging nature of the resistance at negative gate voltage is expected for a depleted 2DES.

$$\frac{1}{R_{Measured}} = \frac{1}{R_{Metal-Overlayer}} + \frac{1}{R_{2DES}} \quad (1)$$

### S2: Role of Ag Capping

To show that absence of superconductivity in co-capped (100) SrTiO<sub>3</sub>/LaAlO<sub>3</sub> interface is not related to ferromagnetism in the cobalt, we used silver (Ag) capping. Ag has low work function and can therefore reduce the critical thickness by increasing the charge transfer. The measured Ag capped (100) interface for 3 monolayers (ML) of LaAlO<sub>3</sub> does not show full superconducting transition for any gate voltage. This confirms that ferromagnetism of Co is not the cause for the absence of superconductivity in (100) co-capped interfaces. In Figure S2 (a) we show the sheet resistance of Ag capped (100)SrTiO<sub>3</sub>/LaAlO<sub>3</sub> as a function of temperature at different positive gate voltages. A dip in the sheet resistance can be attributed due to the localized superconducting regions which are not connected percolatively even on application of positive gate bias. These localized regions may arise from spurious damage from the sputtering or slight thickness nonuniformity. A similar dip has been observed in the Platinum (Pt) capped (100)SrTiO<sub>3</sub>/LaAlO<sub>3</sub> interface for 9 ML of LaAlO<sub>3</sub>. Nevertheless it has been disappeared at strong positive gate bias as shown in Figure S2 (b). The data thus suggest there is no macroscopic superconductivity present in (100)SrTiO<sub>3</sub>/LaAlO<sub>3</sub> interface below the bare criti-

cal thickness upon metal capping.

### S3: Analysis of critical fields

The temperature dependence of the perpendicular and parallel critical fields were analyzed according to the phenomenological Ginzburg-landau theory for the 2-

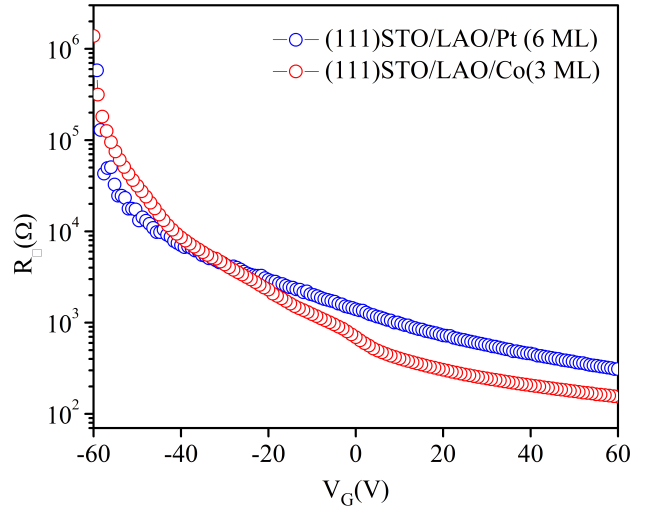


FIG. 5. S1 : The extracted sheet resistance of (111)SrTiO<sub>3</sub>/LaAlO<sub>3</sub>/Co/AlO<sub>x</sub> and (111)SrTiO<sub>3</sub>/LaAlO<sub>3</sub>/Pt samples for 3 and 6 ML of LaAlO<sub>3</sub> as a function of a gate voltages. The resistance was extracted according to the equation 1. The diverging nature of the the resistance at negative gate represents the depletion of the 2DES.

dimensional nature of the superconductivity. The perpendicular and parallel critical fields in the framework of the Ginzburg-landau theory follow equation 2 and 3 respectively. In Figure S3, we show the fit to equation 1 and 2 for (111)SrTiO<sub>3</sub>/LaAlO<sub>3</sub>(3ML)/Co interface. The extracted perpendicular ( $H_{\perp}$ ) and parallel critical field ( $H_{\parallel}$ ) as a function of gate voltages has been shown in Figure 4 of the main text.

$$H_{\perp} = \frac{\phi_0}{2\pi\xi^2} \left(1 - \frac{T}{T_c}\right) \quad (2)$$

$$H_{\parallel} = \frac{\phi_0\sqrt{12}}{2\pi\xi^2d} \left(1 - \frac{T}{T_c}\right)^{\frac{1}{2}} \quad (3)$$

**Table S1:** The extension of table 1 from the main text. Summary of the different samples measured for various thickness of LaAlO<sub>3</sub> upon different metal capping and corresponding nature of the interface.

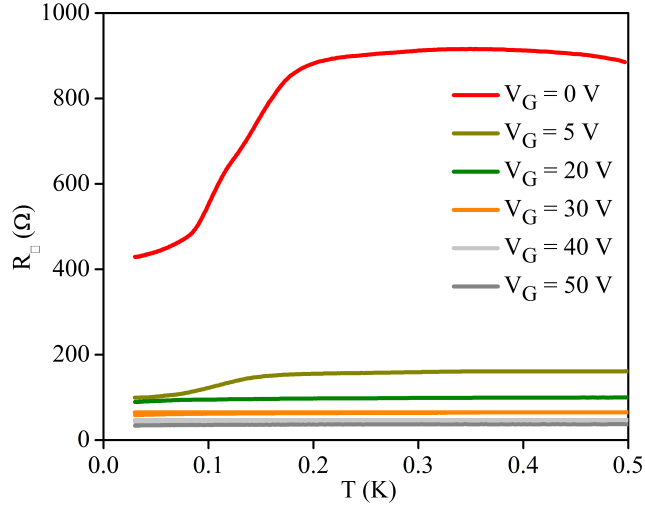


FIG. 6. S2 (a):The sheet resistance of (100) SrTiO<sub>3</sub>/LaAlO<sub>3</sub>/Ag interface for 3 LaAlO<sub>3</sub> ML as a function of temperature at different gate voltages shows an absence of superconductivity. A dip in the resistance can be attributed to the localized superconducting regions which may result from thickness inhomogeneity of LaAlO<sub>3</sub>.

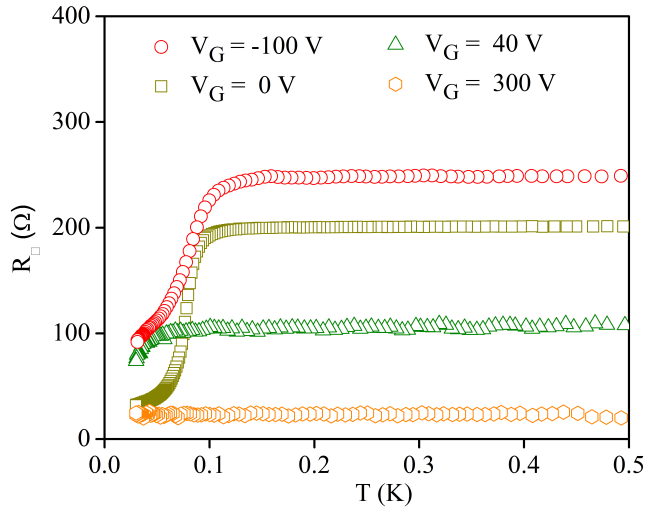


FIG. 7. S2 (b):The resistance of (100) SrTiO<sub>3</sub>/LaAlO<sub>3</sub>/Pt interface for 9 LaAlO<sub>3</sub> ML as a function of temperature at different gate voltages. A partial superconducting transition could be a result of thickness inhomogeneity of LaAlO<sub>3</sub>.

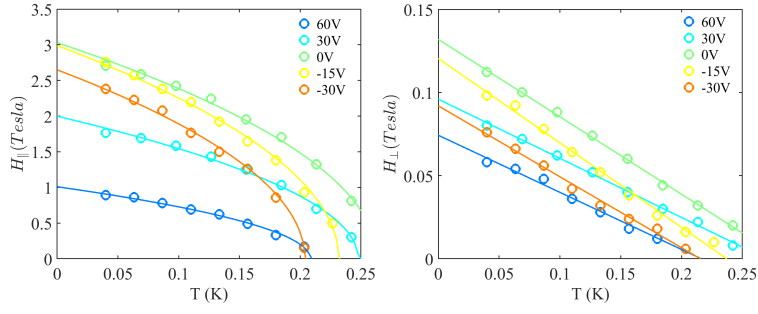


FIG. 8. S3: The perpendicular ( $H_{\perp}$ ) and parallel critical field ( $H_{\parallel}$ ) as a function of temperature for (111)SrTiO<sub>3</sub>/LaAlO<sub>3</sub>(3ML)/Co interface. The solid lines are fit to the equation 2 and 3.

Interface	Metal layer	Thickness (ML)	Conducting	Super-Conducting
(111)	Co	1	No	No
(111)	Co	2	No	No
(111)	Co	3	Yes	Yes
(111)	Co	4	Yes	Yes
(111)	Co	6	Yes	Yes
(111)	Co	7	Yes	Yes
(111)	Pt	5	No	No
(111)	Pt	6	Yes	Yes
(111)	Pt	9	Yes	Yes
(111)	Pt	12	Yes	Yes
(100)	Co	2	Yes	No
(100)	Co	3	Yes	No
(100)	Pt	9	Yes	No
(100)	Ag	3	Yes	No